Vol 17 No 2, February 2008
1674-1056/2008/17(02)/0690-07

Chinese Physics B

© 2008 Chin. Phys. Soc.
and IOP Publishing Ltd

Growth temperature dependent evolutions of microstructural, optical and magnetic properties of $Zn_{0.75}Co_{0.25}O$ films*

Qiu Dong-Jiang(邱东江)[a)†], Feng Chun-Mu(冯春木)[b)], Feng Ai-Ming(冯爱明)[c)], and Wu Hui-Zhen(吴惠桢)[a)]

[a)] *Department of Physics, Zhejiang University, Hangzhou* 310027, *China*
[b)] *Center of Analysis & Measurement, Zhejiang University, Hangzhou* 310028, *China*
[c)] *College of Metrology Engineering, China Institute of Metrology, Hangzhou* 310018, *China*

(Received 23 June 2007; revised manuscript received 3 September 2007)

$Zn_{0.75}Co_{0.25}O$ films are fabricated via reactive electron beam evaporation. The influence of growth temperature on the microstructural, optical and magnetic properties of $Zn_{0.75}Co_{0.25}O$ films is investigated by using x-ray diffraction, selected area electron diffraction, field emission scanning electron microscope, high resolution transmitting electron microscope, photoluminescence (PL), field dependent and temperature dependent DC magnetization, and x-ray photoelectron spectroscopy (XPS). It is shown that $Zn_{0.75}Co_{0.25}O$ films grown at low temperatures (250–350°C) are of single-phase wurtzite structure. Films synthesized at 300 or 350°C reveal room temperature (RT) ferromagnetism (FM), while superparamagnetism for 250°C fabricated films is found above 56 K. PL and XPS investigations show favour towards the perspective that the O-vacancy induced spin-split impurity band mechanism is responsible for the formation of RT FM of $Zn_{0.75}Co_{0.25}O$ film, while the superparamagnetism of 250°C fabricated film is attributed to the small size effect of nanoparticles in $Zn_{0.75}Co_{0.25}O$ film.

Keywords: diluted magnetic semiconductor, ZnO, photoluminescence, magnetic properties
PACC: 7280E, 7550P, 7855E

1. Introduction

Studies on the diluted magnetic semiconductors (DMSs) have attracted much attention since the 1980th.[1,2] The remarkable characteristic of DMSs is that they have both charge and spin degrees of freedom compared with conventional nonmagnetic semiconductors. It is predicted that the realization of new functional DMSs will lead to the advent of new magneto-optic and magneto-electric devices. Normally DMSs are realized by doping 3d transitional metal (TM) into the matrix of III-V or II-VI semiconductors, due to the intrinsical nature of TM that its 3d electronic orbit is not fully occupied. Recently, the research on ZnO-based DMSs is a hot point. This is because the wide band gap of ZnO (3.37 eV) would make it an ideal candidate to realize its ferromagnetism (FM) with a high Curie temperature ($\geq$ 300 K).[3] Also, by utilizing the wide band gap nature of ZnO-based DMSs, transparent magneto-optic devices can be fabricated.[4] So far theoretical results of ZnO-based DMSs reported by different research groups are consistent with each other.[3,4] However, there exists some inconsistency in experimental data from different groups. For instance, Liu *et al*[5] synthesized paramagnetic $Zn_{1-x}Co_xO$ ($x = 0.05$) powders via solid state reaction while Wang *et al*[6] realized room temperature (RT) FM of $Zn_{1-x}Co_xO$ (x = 0.02, 0.06, 0.1) powders by the post-annealing of the sample in H_2 atmosphere. By using the same sol-gel technique, Liu *et al*[7] prepared non-ferromagnetic $Zn_{0.95}Co_{0.05}O$ powder and ferromagnetic $Zn_{0.95}Co_{0.05}O$ thin film. Lim *et al*[8] and Liu *et al*[9] realized RT FM of $Zn_{1-x}Co_xO$ films grown by magnetron sputtering, Tuan *et al*[10] synthesized $Zn_{1-x}Co_xO$ film by metalorganic chemical vapour deposition with its FM remaining up to 350 K, but Jin *et al*[11] reported non-ferromagnetic $Zn_{1-x}Co_xO$ films grown by laser molecular beam epitaxy. It is interestingly found whether the FM is realized in TM doped ZnO is dependent on growth condition. Since the magnetic property of $Zn_{1-x}TM_xO$ film is dependent on its microstructure to a great extent, the microstructure of $Zn_{1-x}TM_xO$ film, which involves the concentration of TM^{2+} dopant (as well as

*Project supported by the National Natural Science Foundation of China (Grant No 50472058).
†E-mail: djqiu@zju.edu.cn

the defects such as O-vacancy and Zn interstitial) and its distribution in the film, is dependent on growth parameters. In this work, a reactive electron beam evaporation (REBE) approach is utilized to fabricate Co-doped ZnO films. The influence of growth temperature on the microstructural, optical and magnetic properties of the $Zn_{1-x}Co_xO$ ($x \approx 0.25$) films is systematically investigated. RT FM is realized in single phase $Zn_{0.75}Co_{0.25}O$ films grown at 300 and 350°C, and the FM origin is also discussed.

2. Experimental details

$Zn_{1-x}Co_xO$ thin films were fabricated on Si(111) wafers which had been polished to a mirror finish and cleaned by REBE technology. Polycrystalline $Zn_{1-y}Co_yO$ ceramic target was used as a source material. The target was prepared in the following way: ultrafine ZnO and Co_2O_3 powders (each with a purity of 99.99%) were blended into a certain atomic ratio of Co:Zn, then the mixture was compressed and finally sintered at 600°C in oxygen atmosphere for 10 h. Growth parameters were kept constant except the substrate temperature, which varied from 250 to 400°C. Background pressure in the growth chamber was 3×10^{-3} Pa. During film growth the high-purity oxygen gas was introduced into the chamber and its partial pressure was set at 2×10^{-2} Pa. The Co content in $Zn_{1-x}Co_xO$ film was surveyed by energy-dispersive spectroscopy (EDS) equipped with S-4700 II field emission scanning electron microscope (FESEM). D/Max IIIB x-ray diffraction (XRD) and selected area electron diffractometer (SAED) equipped with JEM-2010 transmitting electron microscope (TEM) were used to examine the structure of $Zn_{1-x}Co_xO$ films. Alpha-step 200 profilometer was used to measure the thickness and average surface roughness of $Zn_{1-x}Co_xO$ films. RF-540 fluorophotometer was employed to characterize photoluminescence (PL) properties of $Zn_{1-x}Co_xO$ film. In PL measurement a xenon lamp was used as an excitation source and the excitation line was set at 240 nm. Detection energy was scanned from 330 to 650 nm and a filter was used to eliminate the disturbance of excitation source at 480 nm. Field-dependent DC magnetization curves (M-H curves) of $Zn_{1-x}Co_xO$ films were recorded by using Lake Shore 7407 vibrating sample magnetometer (VSM), while the temperature dependent magnetization curves (M-T curves) were measured on a PPMS-9 physical property measuring system. The valence of Co dopant in $Zn_{1-x}Co_xO$ films was investigated by EAC 2000-125 x-ray photoelectron spectroscopy (XPS). XPS was also utilized to evaluate interactions between Co 2p and O 1s core levels in the film.

Firstly, by investigating Co composition in $Zn_{1-x}Co_xO$ films using EDS, we studied the correlation between the Co concentration in $Zn_{1-x}Co_xO$ film, x, and that in $Zn_{1-y}Co_yO$ target, y. Correlation between x and growth temperature or film thickness, was also surveyed. It is found that x is about 2 to 3 times larger than y, and increases only with y increasing, but it is nearly independent of growth temperature or growth duration. For instance, by utilizing $Zn_{1-y}Co_yO$ ($y = 0.1$) target we obtained $Zn_{1-x}Co_xO$ films with x always ranging from 0.24 to 0.26, although the growth temperature varies in a range of 250–400°C and growth duration in a range of 1–2 h. Considering the uncertainty of EDS, which is about 10%, it is presumed that Co concentration in $Zn_{1-x}Co_xO$ film, x, is not obviously influenced by growth temperature and film thickness. So, we regard $Zn_{1-x}Co_xO$ ($x = 0.24$–0.26) films grown from $Zn_{1-y}Co_yO$ ($y = 0.1$) target as $Zn_{0.75}Co_{0.25}O$ in the following sections.

3. Results and discussion

3.1. Growth temperature dependent microstructures of $Zn_{0.75}Co_{0.25}$ O films

Figure 1 shows typical XRD patterns of $Zn_{0.75}Co_{0.25}O$ films fabricated from $Zn_{0.9}Co_{0.1}O$ target. The XRD intensities are in log scale to illustrate whether there exist any impurity phases (such as CoO, $ZnCo_2O_4$ or metallic Co clusters) segregated from $Zn_{1-x}Co_xO$ film. Curves (a), (b), (c) and (d) correspond to the growth temperatures 250, 300, 350 and 400°C, respectively. The alpha-step profilometer measured film thicknesses of samples illustrated in Fig.1 are in a range of 800±20 nm. In XRD curves symbol # denotes the diffraction peak corresponding to ZnO-like wurtzite structure. On the one hand, all peaks in curves (a), (b) and (c) can be indexed as (100), (002), (101), (103), (112) and (004) diffractions of wurtzite $Zn_{0.75}Co_{0.25}O$ without any impurity phases found, which indicates that $Zn_{0.75}Co_{0.25}O$

films grown at low temperatures (≤ 350°C) have ZnO-like structure and thereby suggests that Co ions are substituted mainly for Zn ions sited in the ZnO lattices. On the other hand, $Zn_{0.75}Co_{0.25}O$ films deposited at 250°C have a high degree of *c*-axis orientation and the intensity of (002) diffraction peak is absolutely dominant, as shown in Fig.1(a). It indicates that relatively low substrate temperatures are more advantageous to the realization of highly *c*-axis oriented wurtzite-structured films, which is ascribed to the fact that (001) facet of wurtzite structure has the smallest surface energy. For $Zn_{0.75}Co_{0.25}O$ films deposited at 300 and 350°C, relatively strong intensities of non-(002) peaks, such as (100) and (101), can be found, and they exhibit a typical polycrystalline character as shown in Figs.1(b) and 1(c). Furthermore, it is seen from Fig.1(d) that the further increase of growth temperature leads to the segregation of CoO phase. A similar impurity phase segregation has also been observed in $Zn_{1-x}Co_xO$ films fabricated by pulse laser deposition (PLD) at an enhanced growth temperature[12,13] which may be probably ascribed to the metastable nature of $Zn_{0.75}Co_{0.25}O$ material.

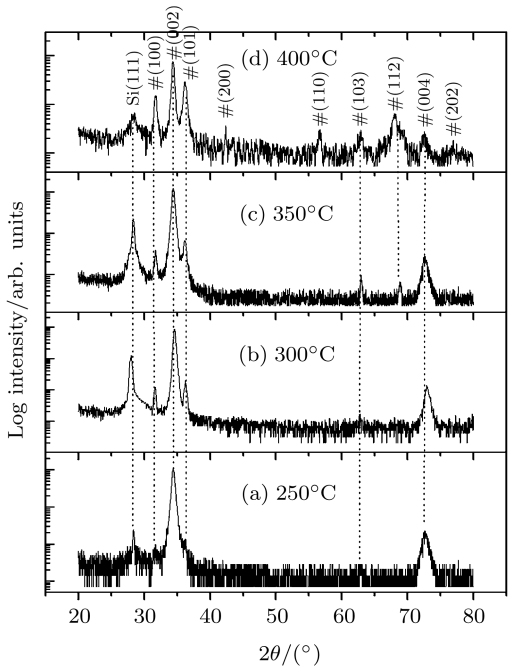


Fig.1. XRD patterns of $Zn_{0.75}Co_{0.25}O$ films grown at 250 (a), 300 (b), 350 (c) and 400°C (d).

Figure 2 shows FESEM images of $Zn_{0.75}Co_{0.25}O$ films grown at different temperatures. It is noticed

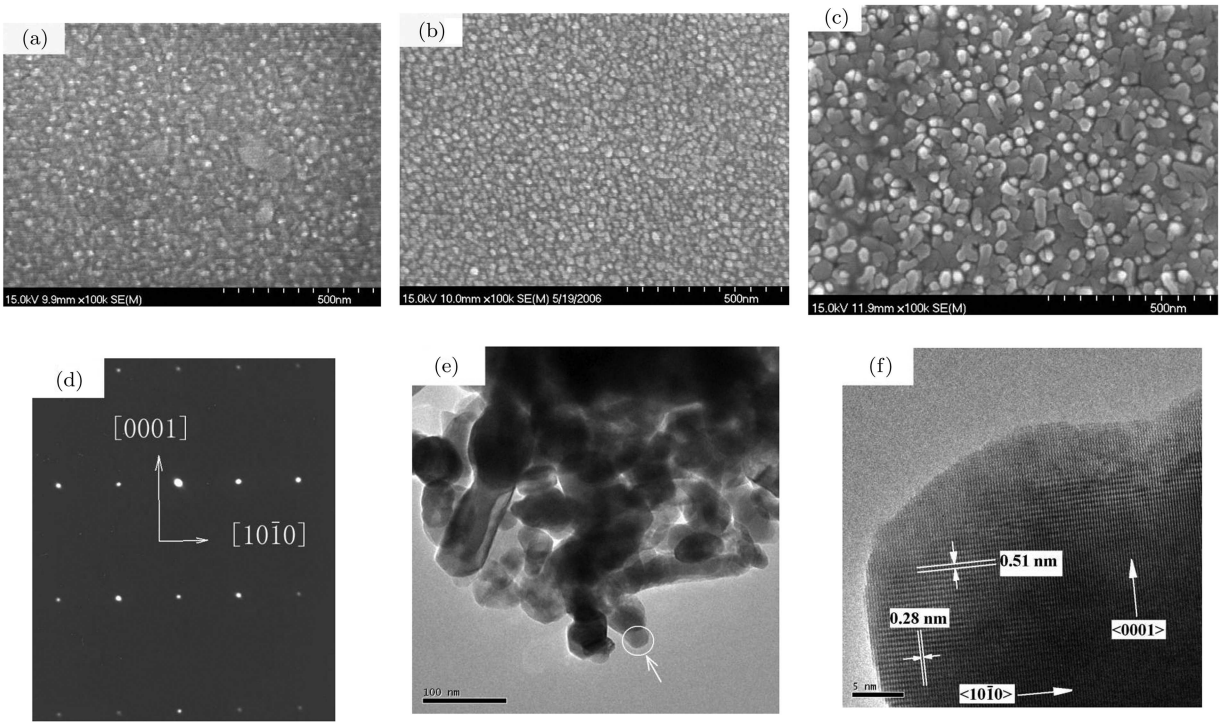


Fig.2. FESEM images of $Zn_{0.75}Co_{0.25}O$ films grown on Si(111) substrates at 250 (a), 300 (b) and 350°C (c), respectively. Images of SAED (d), TEM (e) and HRTEM (f) are taken from the 350°C fabricated $Zn_{0.75}Co_{0.25}O$ sample.

from Figs.2(a) to 2(c) that all of the samples demonstrate smooth surface morphology overall. However, as growth temperature increases, the average size of crystallite in $Zn_{0.75}Co_{0.25}O$ film turns larger and the film surface becomes rougher. The average sizes of crystallites corresponding to Figs.2(a), 2(b) and 2(c) are approximately 15, 20 and 50 nm in diameter, respectively. And the alpha-step profilometer measured average surface roughnesses of $Zn_{0.75}Co_{0.25}O$ films corresponding to Figs.2(a), 2(b) and 2(c) are 3.8, 4.8 and 6.6 nm, respectively.

The microstructure of 350°C fabricated $Zn_{0.75}Co_{0.25}O$ sample was further examined by using SAED, TEM and high resolution TEM (HRTEM), as shown in Figs.2(d), 2(e) and 2(f), respectively. TEM specimen was prepared in the following way. $Zn_{0.75}Co_{0.25}O$ film was detached from the substrate, then the powder-like sample was put into ethanol solution and after an ultrasonic processing the solution turns into suspension. And then the suspension was dropped onto a carbon film, which was supported by a Cu meshwork, for SAED and TEM observations. Figure 2(d) shows the SAED pattern of wurtzite $Zn_{0.75}Co_{0.25}O$ without additional reflections emerging. Figure 2(f) shows the lattice image corresponding to the circled region marked by an arrow in Fig.2(e). Figure 2(f) demonstrates a single crystalline nature of $Zn_{0.75}Co_{0.25}O$ crystallite with its growth direction along [001], which confirms again that Co^{2+} ions are substituted for Zn ions sited in the ZnO matrix and is consistent well with SAED result. The spacing between (001) planes is 0.51 nm as shown in Fig.2(f), which is smaller than that of ZnO lattice ($a = 0.325$ nm, $c = 0.521$ nm), suggests that the tensile stress is introduced into the film when Co^{2+} ions incorporated into ZnO lattice, due to the fact that radius of Co^{2+} ion (0.058 nm) is slightly smaller than that of Zn^{2+} (0.060 nm).[5]

3.2. Optical characteristics of $Zn_{0.75}Co_{0.25}O$ films grown at different temperatures

Figure 3 illustrates a comparison among room temperature PL spectra of $Zn_{0.75}Co_{0.25}O$ samples grown at different temperatures. It is seen from Fig.3 that two strong violet emissions B and C respectively in ranges of 390–397 and 413–430 nm dominate all of the spectra. Besides the two strong emissions, there

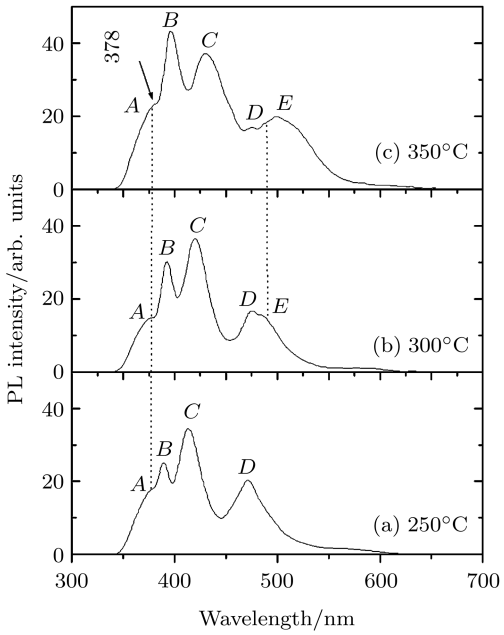


Fig.3. Photoluminescence of $Zn_{0.75}Co_{0.25}O$ films grown at 250 (a), 300 (b) and 350°C (c).

exist a weak ultraviolet emission A peaked at ∼378 nm and a blue-green emission D at ∼475 nm. The peak at ∼378 nm is ascribed to band-to-band transition of ZnO-like band structured $Zn_{0.75}Co_{0.25}O$. The emission in a range of 390–397 nm originates from radiative annihilation of free excitons of $Zn_{0.75}Co_{0.25}O$ crystal. The emissions in a range of 413–430 and at ∼475 nm are probably related to the bound exciton recombinations and the surface related defects of $Zn_{0.75}Co_{0.25}O$ films, respectively.[14,15] Bound excitons may be confined in ultrafine $Zn_{1-x}Co_xO$ nanoparticles in the film. By making a comparison among curves (a), (b) and (c) in Fig.3 it is found that the relative intensity for free exciton related emission (peak B) turns stronger with the increase of growth temperature, while the bound exciton and the surface defect related emissions (peaks C and D, respectively) become weaker. Such an evolution in PL characteristic is probably attributed to the annealing effect under the condition of higher growth temperatures. It is well known that ZnO has a variety of native defects, and some of them can be removed by annealing. Thus the decrease in the relative intensity of surface related defects might be due to the removal of these defects by annealing. However, it is also found from Fig.3 that O-vacancy related emission (peak E at about 485–500 nm)[16,17] gradually emerges and is red-shifted with the growth temperature increasing from 250 to 350°C as shown by curves (b) and (c). The stronger intensity and larger red-shift of the emission

at ∼500 nm indicated by curve 3(c) than those shown by curve 3(b) imply that there exist a larger number of O-vacancies in $Zn_{0.75}Co_{0.25}O$ film grown at 350°C. It is believed that relatively high growth temperature is an essential reason for introducing a large number of O-vacancy defects into $Zn_{0.75}Co_{0.25}O$ film, because the higher temperatures result in the desorption of O-atom from the growing surface of $Zn_{1-x}Co_xO$ film.

3.3. Room temperature ferromagnetism and its origin for $Zn_{0.75}Co_{0.25}$ O films grown at 300 and 350°C

Figure 4 shows VSM measured RT M-H curves of $Zn_{0.75}Co_{0.25}O$ samples fabricated at 250 (a), 300 (b) and 350°C (c), respectively. Although the measured

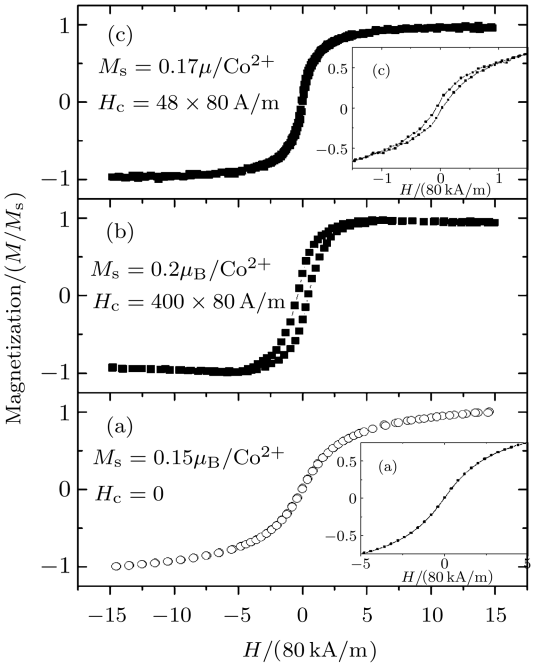


Fig.4. Room temperature M-H curves for $Zn_{0.75}Co_{0.25}O$ films grown at 250 (a), 300 (b) and 350°C (c), with the applied field being parallel to the film surface. The insets (a) and (c) are for the enlarged parts corresponding to curves (a) and (c), respectively.

saturation magnetization (M_s) is only in a range of 0.15–0.2 μ_B/Co^{2+} as summarized in Table 1, it is evident from Figs.4(b) and 4(c) that $Zn_{0.75}Co_{0.25}O$ films grown at 300 and 350°C are ferromagnetic. Moreover, it is found that the RT M_s, as well as the remanence (M_r) and the coercive force (H_c) undergoes a dramatic change depending on growth temperature. Specifically, the RT M_s, M_r and H_c first increase with growth temperature increasing from 250 to 300°C, then decrease with growth temperature further increasing from 300 to 350°C, as summarized in Table 1. By taking FESEM results into account, it is deduced that the average size of $Zn_{0.75}Co_{0.25}O$ nanoparticles grown at 300°C (approximately 20 nm in diameter, as shown in Fig.2(b)) is closer to the critical size of single domain particle of $Zn_{0.75}Co_{0.25}O$ material. This is because nanoparticles are energetically unfavorable for forming domain wall and below a certain size, depending on material, and they prefer to stay in a single domain configuration. For a single domain particle, magnetization reversal can occur only by magnetization rotation as opposed to the combination of domain wall motion with magnetization rotation for a multi-domain particle. Since the magnetization rotation requires work to be done against the strong anisotropy forces, single-domain particle needs a higher field to switch over its magnetization and hence has a larger H_c.[18] Therefore, the closer to its critical size of single domain particle the size of a magnetic particle is, the larger its H_c will be.

Table 1. M_s, M_r and H_c values of room temperature $Zn_{0.75}Co_{0.25}O$ film as a function of growth temperature (T).

T/°C	$M_s(\mu_B/Co^{2+})$	$M_r(M_r/M_s)$	H_c(80 A/m)
350	0.17	0.02	48
300	0.20	0.32	400
250	0.15	0	0

On the other hand, it is seen from Fig.4(a) and Table 1 that both M_r and H_c of 250°C fabricated $Zn_{0.75}Co_{0.25}O$ film are zero, demonstrating a typical superparamagnetic characteristic, which is consistent with the fact that the average crystallite size of 250°C fabricated $Zn_{0.75}Co_{0.25}O$ film (about 15 nm in diameter) is even smaller than that of 300°C fabricated sample as shown in Figs.2(a) and 2(b). Since for a single domain particle the easy directions of magnetization are separated by an anisotropic barrier K_1V, where K_1 is the first-order magnetocrystalline anisotropy constant and V is the particle volume. If the particle size is sufficiently small, the thermal fluctuations at temperatures above a certain temperature (the blocking temperature, T_B) would dominate and the particle can spontaneously switch over its magnetization from one easy axis to another. Such a system of superparamagnetic particles does not show any hysteresis be-

haviours in the M-H curves above T_B, hence H_c and M_r are zero. It is noted that T_B of 250°C fabricated nanocrystalline $Zn_{0.75}Co_{0.25}O$ film is ~56 K, which is determined by zero-field-cooled (ZFC) and field-cooled (FC) M-T curves measured at a field strength of 40000 A/m as shown in Fig.5. Furthermore, from FC M-T curve, we obtain $1/M$-T curve as shown in the inset in Fig.5. It is found that in a range of about 75–300 K the $1/M$-T curve obeys the Curie-Wise's law, $\frac{M}{H} = \frac{C_0 x}{T - \Theta_0 x}$, with a negative Curie-Wise temperature (Θ_0), suggesting that except the ferromagnetic exchange interaction between substituted Co^{2+} ions there exists an anitferromagnetic exchange interaction between some of neighbouring Co^{2+} ions. However, the Curie-Wise's law fitted Θ_0 is evaluated only to be –5 K, much smaller than that of PLD fabricated $Zn_{1-x}Co_xO$ film (where $\Theta_0 = -810$ K),[12] implying that in a REBE fabricated $Zn_{0.75}Co_{0.25}O$ film system the ferromagnetic exchange interaction between substituted Co^{2+} ions is much more dominant than that of anitferromagnetic exchanges.

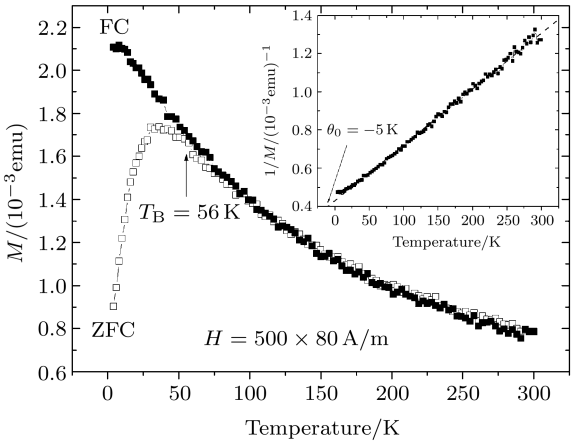


Fig.5. Temperature dependent magnetization curves of 250°C fabricated $Zn_{0.75}Co_{0.25}O$ film under the ZFC and FC conditions. The applied static field is 40000 A/m along the film plane. The inset shows the $1/M$-T curve corresponding to FC curve.

It is known that the critical volume of the superparamagnetic particle can be obtained from

$$\frac{1}{\tau} = f_0 \cdot \exp\left(-\frac{K_1 V}{k_B T_B}\right), \qquad (1)$$

where τ is the relaxation time of a certain magnetic particle, f_0 is the frequency factor, k_B is the Boltzmann constant, T_B is the blocking temperature, K_1 is the magnetocrystalline anisotropy constant and V is the critical volume of the superparamagnetic particle, given by $V = \frac{1}{6}\pi D^3$ in the spherical approximation, with D being the diameter of the spherical particle. For the $Zn_{0.75}Co_{0.25}O$ particle film with grains of an average particle diameter $D = 15$ nm and blocking temperature $T_B = 56$ K, when $\tau = 100$ s and $f_0 = 10^9$ Hz, then K_1 is evaluated to be 1.1×10^4 J/m^3. Obviously, such a magnitude of K_1 is more than 20 times smaller than that of metallic Co material (for bulk Co, $K_1 = 2.7 \times 10^5$ J/m^3[19]). The small K_1 of $Zn_{0.75}Co_{0.25}O$ compared with that of metallic Co implies again that the doped Co^{2+} ions are substituted for Zn ions sited in ZnO lattices.

Figure 6 shows a comparison between XPS curves for Co 2p and O 1s core electrons of $Zn_{0.75}Co_{0.25}O$ films grown at different temperatures. The Co 2p and

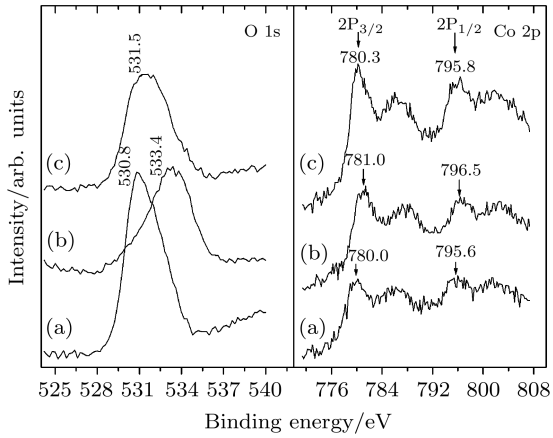


Fig.6. XPS curves for Co 2p and O 1s core levels of $Zn_{0.75}Co_{0.25}O$ films grown at 250 (a), 300 (b) and 350°C (c).

O 1s curves each have been calibrated by using the simultaneously measured Zn 2p peak of the same sample. It is seen from Fig.6 that Co $2P_{3/2}$ peaks for curves 6(a), 6(b) and 6(c) are located at 780.0, 781.0 and 780.3 eV, respectively. The spacings between $2P_{3/2}$ and $2P_{1/2}$ peaks for curves 6(a), 6(b) and 6(c) are 15.6, 15.5 and 15.5 eV, respectively. Because the peak positions of $2P_{3/2}$ core level for Co and Co^{2+} are located at 777.9 and 780.0 eV, the binding energy spacings between $2P_{3/2}$ and $2P_{1/2}$ for Co and Co^{2+} are 15.05 eV and 15.5 eV, respectively.[20] Obviously all of the peak positions of Co $2P_{3/2}$ and the spacings between $2P_{3/2}$ and $2P_{1/2}$ are consistent with those of Co^{2+} as shown in Fig.6, which implies that the valence

of Co in $Zn_{0.75}Co_{0.25}O$ films is +2. Therefore, such a hypothesis that RT FM of $Zn_{0.75}Co_{0.25}O$ films grown at 300 and 350°C originates from metallic Co clusters can be excluded. Furthermore, by making a comparison among curves 6(a), 6(b) and 6(c), one can find that there exist blue-shifts in O 1s and Co 2p peaks for curves (b) and (c), in contrast with curve (a). It should be noted here that the peak position of O 1s for curve (a) is nearly the same as that of ZnO nanomaterial without Co doped.[21] It is believed that the larger blue-shifts of O 1s and Co 2p peaks for curves 6(b) just manifest stronger interactions between O^{2-} of host ZnO and localized Co^{2+} dopants, involving the interaction between O 2p and Co 3d states. Coey *et al*[22] proposed a spin-split impurity band model to interpret the origin of ferromagnetism in DMS materials. The density of unoccupied states for O 2p-Co 3d hybridization is closely related to the interaction between the impurity-band mediated magnetic moments of Co^{2+} ions to give the ferromagnetic state. Therefore, by taking PL and FESEM results into account, it is deduced that the realization of RT FM for $Zn_{0.75}Co_{0.25}O$ films grown at 300 and 350°C is due to the O-vacancy induced spin-split impurity band mechanism predicted by Coey *et al*,[22] while the realization of larger M_s and H_c for 300°C fabricated sample originates from the small size effect of $Zn_{0.75}Co_{0.25}O$ crystallites.

4. Conclusions

$Zn_{0.75}Co_{0.25}O$ films are fabricated via a REBE approach. The influence of growth temperature on the microstructural, optical and magnetic properties of $Zn_{0.75}Co_{0.25}O$ films is systematically investigated by using XRD, SAED, FESEM, HRTEM, PL, XPS, field dependent and temperature dependent DC magnetization measurements. It is shown that $Zn_{0.75}Co_{0.25}O$ films grown at low temperatures (250–350°C) are of single-phase wurtzite structure, but those films that are grown at a higher temperature (400°C) turn inhomogeneous. $Zn_{0.75}Co_{0.25}O$ films grown at 300 and 350°C reveal room temperature ferromagnetism. But 250°C fabricated film shows superparamagnetism above 56 K, which is attributed to the small size effect of nanoparticles in the film. The magnetocrystalline anisotropy constant K_1 of $Zn_{0.75}Co_{0.25}O$ is estimated to be $1.1 \times 10^4\,J/m^3$, which is about 20 times smaller than that of metallic Co material. XPS measurements reveal that the valence of Co in single-phase $Zn_{0.75}Co_{0.25}O$ films is +2. The combined PL and XPS measurements and the K_1 calculation for $Zn_{0.75}Co_{0.25}O$ material show favour towards the perspective that the realization of RT FM of $Zn_{0.75}Co_{0.25}O$ films is duo to the O-vacancy defect induced spin-split impurity band mechanism.

References

[1] Furdyna J K 1988 *J. Appl. Phys.* **64** R29

[2] Gregg J F, Petej I, Jouguelet E and Dennis C 2002 *J. Phys. D: Appl. Phys.* **35** R121

[3] Dietl T, Ohno H, Matsukura F, Cibert J and Ferrand D 2000 *Science* **287** 1019

[4] Wu J J, Liu S C and Yang M H 2004 *Appl. Phys. Lett.* **85** 1027

[5] Liu X C, Shi E W, Song L X, Zhang H W and Chen Z Z 2006 *Acta Phys. Sin.* **55** 2557 (in Chinese)

[6] Wang Y, Sun L, Han D D, Liu L F, Kang J F, Liu X Y, Zhang X and Han R Q 2006 *Acta Phys. Sin.* **55** 6651 (in Chinese)

[7] Liu X C, Shi E W, Chen Z Z, Zhang H W, Zhang T and Song L X 2007 *Chin. Phys.* **16** 1770

[8] Lim S W, Hwang D K and Myoung J M 2003 *Solid State Commun.* **125** 231

[9] Liu X J, Song C, Zeng F, Wang X B and Pan F 2007 *J. Phys. D: Appl. Phys.* **40** 1608

[10] Tuan A C, Bryan J D, Pakhomov A B, Shutthanandan V, Thevuthasan S, McCready D E, Gaspar D, Engelhard M H, Rogers J W, Krishnan K, Gamelin D R and Chambers S A 2004 *Phys. Rev.* B **70** 054424

[11] Jin Z, Fukumura T and Kawasaki M 2001 *Appl. Phys. Lett.* **78** 3824

[12] Kim J H, Kim H, Kim D, Ihm Y E and Choo W K 2002 *J. Appl. Phys.* **92** 6066

[13] Schaedler T A, Gandhi A S, Saito M, Rühle M, Gambino R and Levi C G 2006 *J. Mater. Res.* **21** 791

[14] Wu L, Wu Y and LÜ W 2005 *Physica* E **28** 76

[15] Qiu D J, Yu P, Jiang Y T and Wu H Z 2006 *J. Mater. Sci. Technol.* **22** 541

[16] Vanheusden K, Warren W L, Seager C H, Tallant D R, Voigt J A and Gnade B E 1996 *J. Appl. Phys.* **79** 7983

[17] Zhao J L, Li X M, Zhang S, Yang C, Gao X D and Yu W D 2006 *J. Mater. Res.* **21** 2185

[18] Stoner E C and Wohlfarth E P 1948 *Philos. Trans. R. Soc. London, Ser.* A **240** 599

[19] Yang T L, Shen C M, Du S X, Su Y K, Wang Y G, Wang Y P and Gao H J 2003 *Acta Phys. Sin.* **52** 3114 (in Chinese)

[20] Wagner C D, Riggs W M, Davis L E and Moulder J F 1979 *Handbook of X-ray Photoelectron Spectroscopy*, edited by G E Mulenberg (Perkin-Elmer), p.78

[21] Qiu D J, Yu P and Wu H Z 2005 *Solid State Commun.* **134** 735

[22] Coey J M D, Venkatesan M and Fitzgerald C B 2005 *Nat. Mater.* **4** 173